Spatio-temporal Patterns of T Cell Traction Forces Depend on Stimulation and Cell Subtype

Farah Mustapha [1,2,3,4,5], Martine Biarnes-Pelicot [1,2,3,4], Remy Torro [1,2,3,4,5], Jana El Husseiny [1,2,3,4], Kheya Sengupta [4,5,*], Pierre-Henri Puech [1,2,3,4,*]

Affiliations:

Laboratoire Adhésion et Inflammation (LAI)

[1] Aix Marseille University, LAI UM 61, Marseille, F-13288, France.

[2] Inserm, UMR 1067, Marseille, F-13288, France.

[3] CNRS, UMR 7333, Marseille, F-13288, France.

CENTURI

[4] Turing Center for Living systems, Marseille, France

Centre Interdisciplinaire de Nanoscience de Marseille (CINAM)

[5] AMU CNRS CINaM UMR 7325, Marseille, F-13288, France

[*] To whom correspondence should be addressed :

kheya.sengupta@cnrs.fr, pierre-henri.puech@inserm.fr

Abstract T cells exert forces to sense mechano-chemical cues from their target cells. These forces are feeble and are influenced by environmental factors; as a result, they have often been measured under non-physiological stimulation. Furthermore, a full description of the dynamics of force onset is still missing. Here we investigate the early interaction of T cells with specifically activating ultra-soft hydrogels, which mimic target cells with physiologically relevant stiffness of 350-450 Pa. We quantify the dependence of cell spreading and stiffness on gel elasticity, and measure the morphodynamics of early time traction stresses. The time evolution of the strength of traction forces is quantified as the total elastic energy stored in the gel, and the spatial orientation is characterized via the Cauchy stress tensor. We show that T cells generate stresses in distinct spatio-temporal patterns, which can be sorted into 3 categories: random active-noise, localized intermittent-stress, or a sigmoidal energy-time curve arising from a dipole-like spatial pattern which is usually extensile, and rarely contractile. The relative proportion of cells in each category is condition and T cell subtype dependent. The pattern categories likely reflect the way in which the cell interacts with the target *via* distinct and variously deployed actin-based protrusions. In primary human T cells, the subtype and initial state of the cells strongly impact the relative proportions in each category, in a way that appears coherent with their physiological role. A single metric, which averages the stresses over space and time, fails to capture the stimulation/subtype dependent force application that may be biologically relevant for cell function.

Significance statement The very first step of acquired immunity depends on recognition of pathogenic peptides by T cells using their special T cell receptors. This process relies on application of forces by the cell, which we measure. These measurements reveal hitherto unknown traction dynamics that is not only ligand and stiffness dependent, but also Primary T cell subtype dependent. We propose mechanisms of force application whereby early filopodia generated feeble forces evolve, depending on condition and cell subtype, into intermittent or sustained lamellipodia generated stress that can be extensile or contractile. We hypothesize that these different modes of force application may be linked to the specific physiology of the T cell subtype.

1 Introduction

T cells are activated when the membrane-bound T cell receptors (TCRs) recognize foreign antigenic peptides presented by the major histocompatibility complexes (pMHCs) of antigen-presenting cells (APCs). This happens within a small cell-cell contact area called the immune synapse (IS) (Grakoui et al. 1999; Monks et al. 1998; Reichardt et al. 2010). This interaction bridges the innate and adaptive immune responses. As the activated T cells multiply, depending on their sub-type, they further turn into cytotoxic T cells that directly kill virus-infected and cancer cells, or into helper/regulatory T cells both of which activate and tune the effector functions of other cells in the immune system. There is a growing realization, ever since the pioneering experiments a decade ago, that functions of T cells are highly related to their ability to feel, generate, and respond to forces (Chen et al. 2017; Huse 2017; 2025)

Force response is well-studied in many other cell types, notably tissue-forming cells such as fibroblasts (Elosegui-Artola et al. 2016; Engler et al. 2006; Geiger and Bershadsky 2001; Pelham and Wang 1997; Solon et al. 2007), where it was shown that force is transmitted through well-defined adhesion structures such as focal adhesions, and has an impact on virtually all aspects of cellular physiopathology (Geiger et al. 2009; Janmey et al. 2009; Martino et al. 2018; Schwarz and Safran 2013; Vogel and Sheetz 2006).

Immune cells, such as T cells, do not form focal adhesions *per se*, but their ability to generate and respond to forces is at the heart of their function in a variety of situations, ranging from phagocytosis (Herant 2006; Jaumouillé and Waterman 2020; Vorselen et al. 2021; 2020) and stop/go signal for migration of leukocytes (Huse 2017; Jannat et al. 2011; Kim and Hammer 2021), to antigen extraction and maturation by B cells (Kumari et al. 2019; Spillane and Tolar 2018) and early activation of T cells (Hu and Butte 2016; Klotzsch and Schütz 2013; Liu et al. 2016; Thauland et al. 2017). Recent studies show that T cells respond to forces acting at both molecular and cellular scales, and at timescales ranging from seconds to minutes, with outcomes spread over hours (Basu and Huse 2017; Huse 2017; Limozin and Puech 2019; Puech and Bongrand 2021).

At the molecular scale, the modification of the kinetics properties of the pMHC-TCR bond under force is thought to be implicated in its ability to distinguish different peptidic antigens (Chen et al. 2017; Puech and Bongrand 2021). Specifically, bond lifetime (Ju et al. 2017), rather than the rupture force (Puech et al. 2011), emerges as a potential key parameter, consistent with the TCR/pMHC molecular bond *per se* being a slip, rather than a catch bond (Limozin et al. 2019; Wahl et al. 2019; Liu et al. 2021).

The importance of immune and target cells mechanics at the cell scale has also been documented (Saitakis et al. 2017; Hivroz and Saitakis 2016; Judokusumo et al. 2012; O'Connor et al. 2012; Wahl et al. 2019; Babich et al. 2012). Specific mechanical features of immune cells, in particular APCs, are modulated as a function of the inflammatory conditions (Bufi et al. 2015), and T cells are capable of probing and reacting to this modulation (Judokusumo et al. 2012; O'Connor et al. 2012; Wahl et al. 2019). Interestingly, T cells have also been shown to sense resistance to forces *parallel* to their membrane plane, thus being able to respond to ligand mobility (Comrie et al. 2015; Dillard et al. 2014; Jankowska et al. 2018) as well as readily modulate their global viscoelastic properties in response to local specific signals at very short time scales compared to the calcium fluxes ones, a hallmark of internal signal transduction (Zak et al. 2021).

Traction force microscopy (TFM) has been used to measure cell-scale forces in leukocytes (Henry et al. 2015; Hui et al. 2015; Hui and Upadhyaya 2017; Kumari et al. 2019; Pathni et al. 2022; Ricart et al. 2011), including proof-of-principle measurements on T cells using antibody stimulation in addition to nonspecific interactions to enhance adhesion (Hui et al. 2015; Pang et al. 2024). TFM on T cells is particularly challenging when performed in near-physiological conditions (Mustapha et al. 2022). This is partly because they lack specialized adhesion structures such as focal adhesions, and usually have short contact interaction times with cognate surfaces. T cell traction elicited by purely specific interactions is expected to be low in forces / intensity and deployed on small, ill-defined contact zones as compared to large fibroblast or epithelial cells. Furthermore, from a physiological point of view, T cells are very reactive cells and may exist in different initial states, ranging from naive to anergized (i.e., non-reactive state) as a function of their biomechanical history. As a consequence, force amplitude and patterns may differ even within a given cell population. In an effort to meet the challenge, T cell forces and their spatial distribution have been measured using DNA-force probes (Liu et al. 2016; Ma et al. 2019) and new refined TFM modes are being developed (Lee et al. 2024; Li et al. 2021; Vorselen et al. 2020). Nevertheless, these are yet to be used to their full potential to reveal physiologically relevant force application, especially dynamics of the early recognition events.

Here we used TFM to measure stresses exerted by T cells during the first 15 min of spreading on well-characterized polyacrylamide gels (PAGs) of variable elasticity ranging from ultra-soft (400 Pa) to semi-hard (200 kPa) (Mustapha et al. 2022). We follow, in real-time, the magnitude, and direction of the stresses generated during the first minutes of T cell engagement with the softest gels whose stiffness is similar to that of non-activated DCs and B cells (Bufi et al. 2015). The T cells are

specifically engaged *via* the CD3 domain of the TCR complex, in the optional presence of antibodies against selected co-receptors. We quantify spatio-temporal stress evolution and demonstrate the occurrence of distinct patterns, which are shown, using Jurkat cell line, to be stimulation dependent, and, in primary human T cells from peripheral blood, to be T cell subtype dependent.

2 Results and discussion

Adhesion and spreading depend on gel stiffness, T-cell state and sub-type

Glass-supported PAA hydrogels with a Young modulus in the range of 400 Pa – 200 kPa were produced, the softer being mechanically comparable to physiological APCs (Bufi et al. 2015), and were used as targets. The gels were laterally homogeneous across length scales similar to the T cell size and were doped with fluorescent nanobeads as fiducial markers for following substrate deformations. Previously established protocols, derived from (Tse and Engler 2010), were optimized to obtain gels of well-defined and reproducible rigidity **(see SI text and SI Fig. S1 and S2 for details)**. With typical thickness of ~ 80 µm, the gels were thick enough to be both mechanically homogeneous and stable, and thin enough for simultaneous optical microscopy (Mustapha et al. 2022). Immortalized cultured Jurkat T cells (optionally transfected with LifeAct-GFP) or primary T cells (optionally sorted into subsets) were seeded on gels of various rigidity, which were surface grafted with aCD3 (and optionally with additional stimulatory molecules for Jurkat cells).

To estimate the effect of substrate elasticity on cell spreading and mechanics, cells were seeded on nanobead-free gels and allowed to interact with the surface for 20 min (**Fig. 1A)**. The apparent cell area was quantified from transmission or fluorescence (for GFP transfected Jurkat) microscopy images **(Fig. 1B)**, since PAA gels are not amenable to the more accurate surface microscopy such as reflection interference or total reflection microscopy (Wahl et al. 2019). The median of the measured area was weakly, but significantly, dependent on substrate elasticity, the cells having a tendency to spread, on average, more on the softer substrates with rigidity closer to physiological healthy APCs **(Fig. 1C)**. Interestingly, for Primary T cells on a given stiffness (chosen to be 20 kPa), the spread area is state and subtype dependent **(Fig. 1 D)**. Collectively, these observations are in good agreement with our previous results (Wahl et al. 2019; Yuan et al. 2021) where cell spreading behaviour was shown to be biphasic with substrate stiffness.

Cell stiffness is weakly impacted by gel stiffness, and T-cell state or sub-type

The Young modulus of the cells was measured, after 20 min of interacting with the gel surface, by indenting them with a moderate force *via* bead-decorated AFM cantilevers, up to depths of indentation < 1 µm, which represents ~ < 10% of cell diameter **(Fig. 1E, F)**. The measured Young modulus of the order of 100 Pa on gels at physiological range of stiffness is typical for lymphocytes, including Jurkat T cells, murine hybridomas and primary human cells (Cazaux et al. 2016; Sadoun et al. 2021; Zak et al. 2021) **(Fig. 1G, H)**. For Jurkat cells, the value of the Young modulus does not show strong variation with substrate elasticity on gels with lower elasticity **(Fig. 1G)**, which could reasonably indicate that the deformation of the gel under the cells can be neglected (Rheinlaender et al. 2020). Pooling data and averaging within the low elasticity range (2 to 20 kPa), leads to a value of about 100 Pa for cell stiffness. On stiffer gels that do not mimic per se any relevant APC (Bufi et al. 2015) the Young modulus was higher – similar to the effect of relaxing a shape constraint (Sadoun et al. 2021). Nevertheless, the order of magnitude of the Young modulus is still close to the usually reported values, unlike some very high values reported recently using dynamic AFM modes (> 10 kPa, (Jung et al. 2021)). Interestingly, for Primary T cells on a given stiffness (chosen to be 20 kPa), the naïve, stimulated and memory cells show very different elasticities. However, pre-stimulation appears to have little impact on cell stiffness, at least for the memory T cell sub-type **(Fig. 1H)**.

T cells apply stresses in distinct spatio-temporal patterns

Stresses exerted by Jurkat T cells on target gels, as they land and start interacting with the gel, was quantified by monitoring the position of the gel-embedded nanobeads and using previously described open-source tools for analysis (Mustapha et al. 2022; Martiel et al. 2015). No significant nanobead displacement was generated on a control IgG2a (isotype control) surface. On activating aCD3 surface, small but discernible displacements were recorded. By applying particle image velocimetry (PIV) followed by Fourier transform traction cytometry (FTTC), we obtained the time-dependent stress field, which we present as heat-maps with stress-norms, revealing the magnitude, lateral distribution and the local orientation of the stress, for each time point **(Fig. 2A and SI Fig. S3-S5, also see SI text & movies)**.

Visually focusing on purely spatial aspects, the stress distribution/orientation is seen to be either random (seen in about 60% of all cells on aCD3, 400 Pa gel) or dipolar with the forces pointing outwards, that is to say extensile (seen in about 40 % of all cells). Focusing next on quantification of time evolution, two time dependent metrics were defined - the stress-sum-norms, summed over the whole image with space coordinates i,j at timepoint t, $SSN(t)=\sum_{space}|\sigma_{i,j}(t)|$. Considering the maximum SSN over the entire experimental duration, gives the “max-stress-sum” (in Pa), a

convenient single metric per cell (**Fig. 2B**). The sum of the scalar product of the strain $\varepsilon_{i,j}(t)$ and stress $\sigma_{i,j}(t)$ at each reconstituted pixel, called "Energy" (in J), is: $U(t)=\frac{1}{2}\sum_{space}\varepsilon_{i,j}(t)\sigma_{i,j}(t)$. It corresponds to the elastic energy stored in the gel at the timepoint t (Kumari et al. 2019; Butler et al. 2002), which can be further integrated over the experiment-time to give the "integrated energy" (in J.s), characteristic of a given cell (**Fig. 2 C**). Note that to avoid the difficulty of detecting the exact zone of contact of the cell with the PAA substrate, we chose to calculate these parameters over an entire image of constant size, choosen to be slightly larger than the apparent cell diameter (Mustapha et al. 2022).

Background noise corresponds to energies of the order of 10 atto J, measured for cell-less regions or for cells on non-activating surfaces such as IgG2a (passive fluctuation in **Fig. 2D)**. Jurkat cells on activating aCD3 coated surface generate three typical categories of stress-application dynamics (**Fig. 2D).** In the first category, the signal (U) varies around a relatively low value which is nevertheless higher than the noise detected before arrival of cells, reaching up to about 100 atto J (active fluctuation in **Fig. 2D)**. In the second category, the energy U slowly climbs to a high magnitude, of the order of femto J, but then decreases again (intermittent signal in **Fig. 2D)**. In the third category, the energy remains low for a while after a cell lands, and then rapidly climbs to a value whose magnitude is large compared to the small fluctuations visible before the arrival of the cell (sigmoidal signal, **Fig. 2D)**. The energy stays at this high value, of the order of femto J, during the remaining duration of the experiment (15 min). The force application typically starts as early as 20 second after landing (**Fig. 2E**). For a given population and for a given condition, multiple categories may be present. It is therefore useful to characterize the proportion of cells in each category (**Fig. 2F**). Each category exhibits a distinct spatial distribution (**SI Fig S5**), and corresponds to a characteristic integrated energy, with active noise generating the smallest and sigmoidal signal the highest integrated energy (**Fig. 2G**).

Further analysis of the energy U(t) reveals that for cells on passive gel, the distribution can be fitted with a Gaussian, and the Shapiro-Wilk test confirms that the distribution is normal or near-normal **(SI Fig. S6)**. Note that this residual noise is not expected to be of purely thermal origin since the gel is too stiff for thermal fluctuations to be detectable – instead it originates from instrumental noise and analysis errors. On activating gels, the distribution varies from near-Gaussian to highly non-Gaussian, sometimes with multiple grouped events (**SI Fig. S6**). The power-spectrum on activating gels is more complex compared to cell-less or non-activating case (**SI Fig. S7**). For intermediate and sigmoidal signals, new peaks appear at slow time scales. A systematic matching of assigned

time-trace pattern category to a specific power-spectrum proned to be difficult, probably because of limited signal length (15 min) and time resolution (1 frame / 5 s).

The description of spatial distribution and orientation of the traction can be formalized via the Cauchy stress dipole tensor χ *(Ronceray and Lenz 2015; Tanimoto and Sano 2014; Vitiello et al. 2014)*, defined as: $\chi_{|xy|}(t) = \sum_{space} r_x \sigma_y(t)$, where t is time, x and y are the two space dimensions, the summation is over all the points on a given stress map, r is the space vector and σ the stress. The dipole tensor on a surface is a 2x2 matrix expected to be symmetric, with the sign of the diagonal terms giving information about the nature of the dipole – positive implies an extensile dipole and negative a contractile dipole. We diagonalized χ, calculated its Eigen values and plotted the Eigenvalues as a function of time. Parallel inspection of the energy-time traces U(t) and the principle Eigen vectors of the Cauchy dipole tensor $\chi(t)$ reveals that they track each other closely, recapitulating the stress application categories (**SI Fig. S9**). Notably, the positive sign of the principle Eigen vector confirms an extensile force dipole, in agreement with visual observation.

Spatio-temporal stress-patterns depend on substrate mechano-chemistry

The behavior of the Jurkat cells on aCD3 coated substrates with a Young modulus of ~ 400 Pa (B cell like) vs ~ 2 kPa (macrophage like) (Bufi et al. 2015) was compared. The fraction of cells showing intermittent signal was dominant on the more rigid gel **(Fig. 2H).** Consequently, the pooled maximal stress sum and integrated energy were lower in this later case **(Fig. 2I and J).** Sorting of the integrated energies by time-trace category is shown on **Fig. 2K.** These observations underline the necessity of using ultra-soft gels for monitoring the early forces generated by immune cells, and show why using conventional gels with typical stiffness in the range of 2-5 kPa is not optimal.

The impact of additional antibodies against co-receptors CD28 and CD11a (part of the integrin LFA1), was tested (**SI Fig. S8**). It was seen that the distribution of the temporal patterns is co-receptor dependent. The median value of the integrated energy is not affected by the presence of aCD28, whereas it is slightly lowered in the presence of aCD11a. Noting that as expected, the integrated energy is lowest for intermittent signals, the lowering of integrated energy in case of aCD3/aCD11a can be understood in terms of increase in occurrence of active fluctuation regime. The limited impact in presence of aCD28 is reminiscent of our recent observation that aCD28 did not strongly influence the spreading area of the Jurkat T cell line on soft substrates (Wahl et al. 2019), while it could be different for primary cells (Judokusumo et al. 2012). Overall, the differences discernible in the occurrence of the different temporal pattern categories are hidden when looking at max-stress-sum or integrated energy averaged over the entire population (**SI Fig.**

S8 C,D). When the integrated energy for each regime is plotted separately, the influence of co-receptors on the stress dynamics is again evident (**SI Fig. S8 E**).

Moreover, subtle modification of the actin cytoskeleton via LifeAct-GFP, or even labeling the cell membrane via a GFP label changes the distribution of the categories (**see SI text and SI Fig. S11**), underlining the sensitivity of underlying mechanisms.

Spatio-temporal stress-patterns depend on Primary cell subtype

Primary T cells on activating antiCD3 surfaces, sorted into naïve, activated, and memory cells which may be optionally pre-stimulated, recapitulate the three typical categories of the previously observed stress-application dynamics: spatially random active fluctuations, random but localized intermittent signal, and stress dipolar sigmoidal signal, which is usually extensile as before, but, in a few cases, may also be contractile (**SI Fig. S13**)[1]. The statistical properties of the energy U(t) also exhibits same behavior as before (**SI Fig. S14**). Further analysis shows that as expected, both integrated energy and max-stress-sum are higher on stimulating substrates, compared to the control case on IgG2a **(Fig. 3A,B)**. Importantly, both these metric are cell subtype dependent (the integrated energy varying from atto J.s to femto J.s). Both values are the highest for memory T cells that are not pre-activated. Pre-activation appears to lower the maximal applied stress as well as the integrated energy. Naive T cells exert very small stresses, whereas effector cells (interchangeably called stimulated / activated T cells) exert larger forces, resulting in significant maximal stress and integrated energy, which are nevertheless a fraction of the values seen for memory cells.

Next, focusing the distribution of the stress pattern categories, it is seen that the % of cells in each category is different for each subtype **(Fig. 3C)**. It is seen that memory T cells exhibited more sigmoidal and intermittent pattern types, while effector T cells exhibit exclusively intermittent pattern, and naive T cells exhibit both intermittent and active fluctuations. As seen for Jurkat cell, the percentage of cells in the sigmoidal category correlates strongly with the value of integrated energy: for example, unactivated memory T cells exhibit the highest percentage (circa 86%) of sigmoidal curves, as well as higher levels of integrated energy than the other subtypes; naive T cells on the other hand, are more often in the active fluctuation category (25 %) and display the lowest integrated energy (**Fig. 3D**).

---

1 In addition to the three cataloged patterns, for the memory T cell subpopulation, a multi-step sigmoid, counted under sigmoid, was sometimes observed (not shown here)

Similar to Jurkats, the time evolution of the principle eigen value of the stress dipole tensor $\chi(t)$ follows the energy U(t) (**SI Fig. S15**). As before, for most cases of sigmoidal signal, the principle eigen value increases to a large positive value concomitantly with the energy, consistent with extensile, out-ward pushing stress. However, for memory cells, in a few cases the principle eigen value dips to a large negative value concomitant with the rise in energy, consistent with a contractile stress dipole.

Mechanism of stress pattern generation

At early times after encountering a target, T cells are known to interrogate it via filopodia (or microvilli) before taking a decision to spread or not (Pierres et al. 2008; Göhring et al. 2022; Sengupta et al. 2024; Cai et al. 2017; Brodovitch et al. 2013). The active fluctuation category with very feeble, randomly distributed force application can be attributed to such filopodia mediated first tentative contacts. Filopodia generated pushing forces, expected to be of the order of 1 or 2 pN (Bornschlögl 2013; Clarke and Martin 2021), corresponding to a stress of ~ 0.4 Pa in our setup, are one order of magnitude below our measurement threshold. Thus, even if there were some pushing, the generated stress component would be too feeble to measure. Filopodial pulling forces are however stronger and, depending on adhesion and activation state, range from 20 to 2000 pN, corresponding to a stress range of about 4 to 400 Pa in our experiments (Bornschlögl 2013; Iwadate and Yumura 2008; Parr et al. 2019). The maximum local stress measured here varies across T cell subtypes – from 60 Pa for effectors to 200 Pa for activated memory – well-within the estimated range. Filopodia may generate pulling either due to actin de-polymerization induced retraction, or via actin retrograde flow. Considering the expected relative strengths, we attribute the former to active-fluctuation and the latter to intermittent signal (**Fig. 4**). Due to random in-plane orientations possible for filopodia, the resulting stress vectors also have random orientations. One has to note that TFM is not able to truefully characterize the z-component of forces, but only to measure the projection in the x,y planes of the forces, hence reducing the apparent stress magnitude for point like or finger like pushing or pulling action by thin structures.

At late times, for tissue forming cells, cell traction is generally dominated by myosin generated forces. For T cell spreading however, mechanosensing may be myosin independent, and spreading is mediated by actin polymerization, with force being transmitted to the substrate via ligand-receptor bonds that are connected to the actin retrograde flow, a scenario that can be described by a modified clutch model (Dillard et al. 2014; Wahl et al. 2019). Although in such models, depending on chosen parameters, the energy U(t) can be oscillatory or monotonic sigmoidal, the traction is necessarily contractile – never extensile (Alonso-Matilla et al. 2023).

A candidate mechanism for generating extensile stress is friction between the membrane and the substrate, mediated by non-specific bonds formed by membrane bound receptors – somewhat reminiscent of frictionless amoeboid locomotion (Paluch et al. 2016; Bergert et al. 2015). While the stress reported for frictional locomotion were of the order of 0.2 Pa, in our case the local stress can be higher than 200 Pa, indicating either a higher membrane velocity arising from faster actin polymerization triggered by specific stimulation via aCD3, or a higher frictional coupling to the substrate likely due to absence of soft polymer coating here. Unlike the migration case, the cells here are not confined and must offset these stresses at the opposite end, generating a force dipole. A possible equivalent of such outward pushing forces exerted by actin rich structures was reported, though with a different geometry, and on APCs (Husson et al. 2011; Sawicka et al. 2017; Zak et al. 2021). We hypothesize that a similar structure may be forming here that pushes across the gel, generating friction at one pole of the cell with local adhered structures sustaining an equal and opposite force at the opposite pole (**Fig. 4**). The occasional case of contractile forces we measure here are likely to be generated *via* actin retrograde flow as envisaged in the previously described modified clutch model (Dillard et al. 2014; Wahl et al. 2019) (**Fig. 4**).

Biological significance of stress pattern categories

Extensile stresses were reported for keratocytes (Burton et al. 1999), neutrophiles (Henry et al. 2015), and cytotoxic T lymphocytes at very early state of spreading (Basu et al. 2016). In all these cases the cells switched to contractile stresses at late times – a behavior we qualitatively observed in a few cases (**SI Fig. S16**). When the cell is induced to be fully spread thanks to the addition of non-specific adhesive interactions, near-isotropic contractile forces are seen (Hui et al. 2015; Colin-York et al. 2019).

Dynamic force measurement during early adhesion/spreading of immune cells are rare in literature. The closest to our work is measurement of traction forces exerted by naive CD4+ cells on anti-CD3 coated pillars (Bashour et al. 2014). Though the focus was on time averaged measurements at late times (more than 20 min after landing), the reported exemplary cell force time-trace shows sigmoidal increase and saturation at about 15 min. It is stated that in the initial contact phase, the forces are randomly oriented whereas they become contractile at late times. Our experiments, on continuous deformable substrates, focused on early times, capture this random category for naive CD4+ cells, which manifests itself as active noise or intermittent signal. Such random distribution of generated force was also reported for CTLs acting on pMHC and ICAM coated pillars at early

times (Basu et al. 2016). For transfected Jurkat cells on pMHC, such cellular “stick-slip like” behavior has been reported even at late spreading times (Colin-York et al. 2019).

Considering our results in light of previous studies, a model (**Fig. 4**) for the origin of the various stress patterns emerges where active fluctuations, always seen in early times after cell landing on target, correspond to an interrogation of the surface via filopodia/microvilli without strong adhesion, reminiscent of the observations of (Brodovitch et al. 2013). Depending on the level of cell engagement, due to external cues or internal cell state, filopodia may adhere strongly and generate stronger but temporary local stresses giving rise to intermittent signal. The filopodia mediated interrogation may lead to a decision to switch to lamelipodia mediated spreading, such as the one reported in (Dillard et al. 2014; Brodovitch et al. 2015). A period of sustained filopodia based pulling may be necessary for entering a lamellipod dominated regime. One prediction for such filipodia mediated active pulling leading to a decision, where bonds are stretched, broken and reformed, is that on stiffer substrates, bond breaking becomes more prevalent (Alonso-Matilla et al. 2023; Wahl et al. 2019), preventing an efficient spreading decision. It can therefore be expected that more cells exhibit intermittent and/or active noise phase on stiffer gels. This is indeed the case since the distribution of the different stress pattern categories shifts towards more active noise and intermittent signal on 2 kPa as compared to 400 Pa (**Fig. 2H**).

The T cell subtype dependence of the traction dynamics reported here could arise from biological differences. T cell subtypes vary in their surface receptor expression levels, as well as cytoskeletal molecules including actin, talin, and Arp2/3 – which are enriched in memory and effector cells as compared to naïve (Liu et al. 2001; Kaech et al. 2002) leading to lower spreading for naive cells (Thauland et al. 2017) and possibly contributing to the stiffness variation reported here **(Fig. 1H)**. This is consistent with our observation of naive T cells generating least traction.

In addition, the various spatio-temporal traction pattern categories may be linked to the physiological function of the various T cell subtypes. Memory T cells activate and exert a cytokine (CD4+)/cytotoxic (CD8+) response to their cognate pMHCs irrespective of the presence of a costimulatory signal, whereas a naive T cell never undergoes activation and clonal proliferation outside of the lymphoid structures in absence of costimulation from a dedicated APC (Murphy et al. 2022). We hypothesise that the stronger stresses generated by memory T cells, reflective of more cells entering lamelipodia mediated spreading, may be correlated to their ability to undergo activation more easily upon proper signal encounter. Naive T cells may be stuck in filopodia mediated surface interrogation in absence of strong co-stimulation. The somewhat intermediate

behavior of effector cells, may also be linked to their relative readiness to activate and spread (Sengupta et al. 2024).

3 Conclusions

We produced well-controlled PAA gels and characterized their mechanical properties on scales that are compatible with immune cell dimensions and partner cells rigidities. Using TFM, we then quantified the early stresses and explored their spatio-temporal dynamics. Our approach of using soft gels and strictly specific interactions elicited hitherto unreported behavior. We discovered that early T cell traction is exerted in distinct spatio-temporal stress patterns, which can be classified into three categories, each corresponding to a different actin based force generation mechanism. The stress patterns are highly sensitive to external cues and internal cell state. The proportion of cells in a given pattern category depends on specific stimulation, substrate rigidity and T cell subtype, reflecting an underlying mechanism that depends on switch between different geometries of filopodia or lamellipodia mediated spreading. We argue that stress morphodynamics may be correlated with physiological function of the specific T cell subtype, and may reflect the cells ability to proceed from a filopodia mediated interrogation phase with limited stress generation to a lamelipodia mediated spreading or pulling phase with stronger stress generation. Our results provide new insight into early dynamics of mechanotransduction in lymphocytes, and underline its exquisite sensitivity to biophysical and biochemical cues from the microenvironment.

4 Material and methods

Cells. Human Jurkat T cells (clone E6-1, ATCC TIB-152), as a model for lymphocytes, were obtained from ATCC. Primary cells were purified from blood from healthy volunteers obtained through a formalized agreement with the French Blood Agency (Établissement Français du Sang, agreement 2017-7222), after receiving the informed consent of the donors, in accordance with the Declaration of Helsinki. All experiments were approved by the INSERM Institutional Review Board and the Ethics Committee. For cell culture protocols, purification, sorting transfection details and cytometry experiments, please refer to Supplementary Materials.

Polyacrylamide gels. Fabrication, functionalization and characterization of PAGs (mechanical, by Atomic Force Microscopy indentation, and coating homogeneity by fluorescence microscopy) are summarized in the Supplementary Material and more details can be found in (Mustapha et al. 2022).

T cell spreading evaluation. The cells were left to interact with the medium and temperature equilibrated gels for 20 min before image acquisition started. The system was focused just above the gel surface. The obtained images were processed using Fiji/ImageJ (Schindelin et al. 2012) by delineating the contour of the cells to quantify the apparent cell area. All experiments were performed at 37°C.

T cell mechanics using Atomic Force Microscopy. The maximal force to be applied was set at 500 pN for cells, leading to indentation depths of the order of one µm for cells, using a contact duration of 0 s and the speed of pressing and pulling was 2 µm/s. Data was typically recorded at 2048 Hz. Up to 5 force curves were recorded for each adhered T cell tested, and the median value used for a given cell. Data processing using JPK Instrument software is described in the Supplementary Materials. To note, we chose to fit over 0.5 µm of indentation to minimize contributions from the nucleus (Sadoun et al. 2021). All experiments were performed at 37°C.

Traction Force Microscopy (TFM). The optical microscope set-up and the parameters used are summarized in the Supplementary Materials and can be found in (Mustapha et al. 2022). Briefly, to measure the traction forces, movies of live T cells and fluorescent beads were acquired typically every 5 s for typically 15 min. All experiments were performed at 37°C.

TFM Data processing. TFM movies were processed using a combination of FijiI/ImageJ and in-house Python 3.8 functions. Image sequence was performed using an in-house Python code rom nanobeads tracking data generated with Trackmate (Tinevez et al. 2017). The PIV and FTTC calculations were performed using modified versions of Q. Tseng set of functions for FIJI/ImageJ (https://sites.google.com/site/qingzongtseng/), with further plotting and calculations (https://github.com/phpuech/TFM). We used the Anaconda Python distribution

(https://www.anaconda.com/). All data analysis was performed on Linux 64 bits machines. The entire procedure is detailed in(Mustapha et al. 2022).

Data visualization and statistics. Data plotting and significance testing were performed on Linux or Windows 64 bits machines using Python, R and/or Graphpad Prism (6 or 7). We used non parametric tests (Kruskal-Wallis / Wilcoxon) by default since our data was observed to be often largely distributed and not gaussian. If not stated otherwise, one data point corresponds to one measurement, that is, either one median value for a gel or a cell (AFM), or the one value calculated for a cell (spreading, TFM). We used ns for $P > 0.05$, * for $P \leq 0.05$, ** for $P \leq 0.01$, *** for $P \leq 0.001$ and **** for $P \leq 0.0001$.

Acknowledgments

Part of this work was supported by institutional grants from INSERM, CNRS and Aix-Marseille University to the LAI and CINAM. FM was supported by a PhD grant from the European Union's Horizon 2020 research and innovation program under the Marie Skłodowska-Curie grant agreement 713750, with the financial support of the Regional Council of Provence-Alpes-Côte d'Azur and with of the A*MIDEX (ANR-11-IDEX-0001-02), funded by the Investissements d'Avenir project funded by the French Government, managed by the French National Research Agency (ANR). RT was supported by a PhD grant from CENTURI (Turing Center for Living systems, Marseille, France), funded from the « Investissements d'Avenir » French Government program managed by the French National Research Agency (ANR-16-CONV-0001) and from Excellence Initiative of Aix-Marseille University - A*MIDEX. Q. Tseng is acknowledged for his help in using his set of Image J macros, under the form of a shared project in the frame of the CENTURI engineer platform. We thank L. Limozin, P. Pierobon, M. Balland, A. Nicolas and H. Delanoé-Ayari for extremely helpful discussions, T.-T. Nguyen and the INSERM Cell Culture Facility (PCC, Marseille), P. Ronceray for introducing us to the dipole tensor, C. Hivroz, Y. Hamon and L. Limozin for careful reading and commenting of the manuscript.

Contributions

FM planned and performed the experimental work, analyzed the data and wrote the article, with the help of JEH for primary cell spreading and mechanics. MPB did all cell constructs and helped for cell maintenance and FACS analysis. RT implemented the refined alignment procedure used in the analysis. KS and PHP designed the study, performed some experiments, implemented novel analysis and wrote the article. All co-authors edited the manuscript.

The authors declare no competing interests.

Figures captions

Fig. 1: T cell spreading and mechanical properties on gels A: Schematics of the spreading experiments on antiCD3 coated gels of controlled rigidity, the blue zone indicates the focal plane position to measure the cell's apparent contact area. B: Micrograph of a LifeAct-GFP cell showing the presence of cellular extensions. C: Quantification of the apparent area of Jurkat cells on the different substrates (note that this area is *not* the adhesion area per se but rather, a projected cell area). Typically ~ 200 cells were imaged per condition. D: Spreading of primary T cells on 20 kPa gel as a function of their subtype. E: Schematics of the AFM indentation experiments on cells adhered on similar substrates as for spreading experiments. F: Micrograph showing the bead (white round spot) glued on the cantilever (dark gray triangle) in close proximity to a cell. G: Young modulus measurements of Jurkat cells as a function of substrate rigidity. The Young modulus could not be measured correctly on cells adhered on the softest substrate (see text). H: Young modulus of primary T cells on 20 kPa gel as a function of their subtype. Typically ~20 cells were used per condition.

Fig. 2: Traction Force Microscopy, method and measurement on early Jurkat T cells. A: TFM experiment schematics, with the reference image taken before cell landing. Example sequences, during a Jurkat T cell spreading on a aCD3 coated gel, of calculated movement of the gel embedded nano-beads (by PIV, see Material and methods) and resulting stresses (by FTTC, see Material and methods) B: Max-stress-sum of Jurkat cells interacting with aCD3 vs isotype control antibody showing the specificity of the interaction. C: Corresponding integrated energy. D: Time traces of the energy showing the typical temporal patterns observed in absence (top panel) or presence (bottom 3 panels) of specific cellular interaction. E: Quantification of the standard deviation (SD) of the energy U(t) for different stimulations, before and after landing of cells. Before cell landing and on IgG2a, SD is lower than for cells on aCD3. F: Relative occurrence of the stress pattern categories for cells on IgG2a and aCD3. G: Integrated energy for the different stress pattern categories for cells on aCD3 substrates. H: Relative occurrence of the stress pattern categories for cells on gels of different rigidities coated with aCD3. Color code is the same as in Fig. 2F. I: Pooled max-stress-sum and J: pooled integrated energy for cells on these gels. K: Same data separated by category and gel rigidity.

Fig. 3 : Traction Force Microscopy of primary human cells A: Pooled max-stress-sum as a function of primary T cell subtype. B: Pooled integrated energy. Each point corresponds to a cell, the bar presents the median of the data. C: The relative occurrence of the different stress categories obtained for the displayed T cell subsets. D: Separation of the different categories for the different T cell subsets.

Fig. 4 : Overview of the stress application patterns and proposed modes of interaction Columns are regime types - from left to right - active noise, intermittent, two types of sigmoidal signal. Rows depict - from top to bottom - sketch of signal type with typical order of magnitude of the maximal value indicated, sketch of stress distribution and direction with typical absolute value or range indicated, and cartoon of mechanism of stress application. The stress regimes occur due to switch between different geometries of filopodia or lamellipodia mediated spreading. These regimes may be correlated with physiological function of the specific T cell sub-set.

Graphical abstract

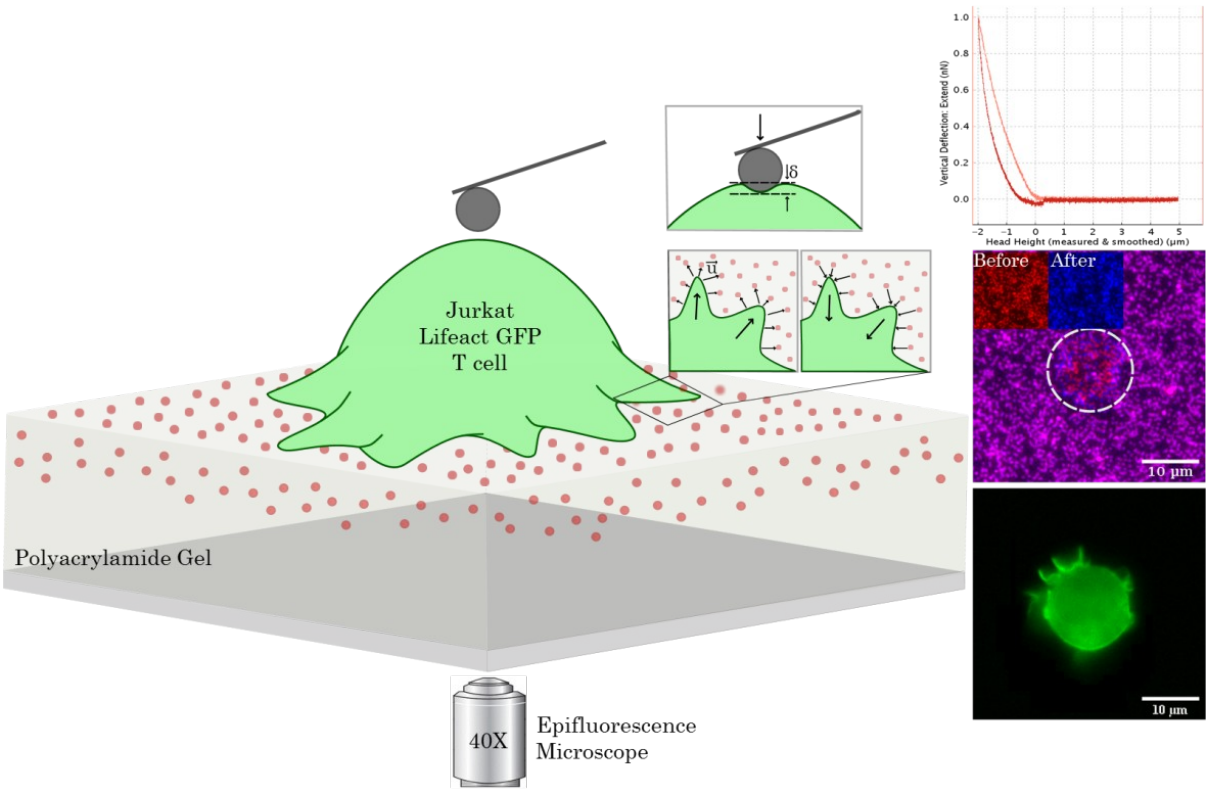

Figure 1

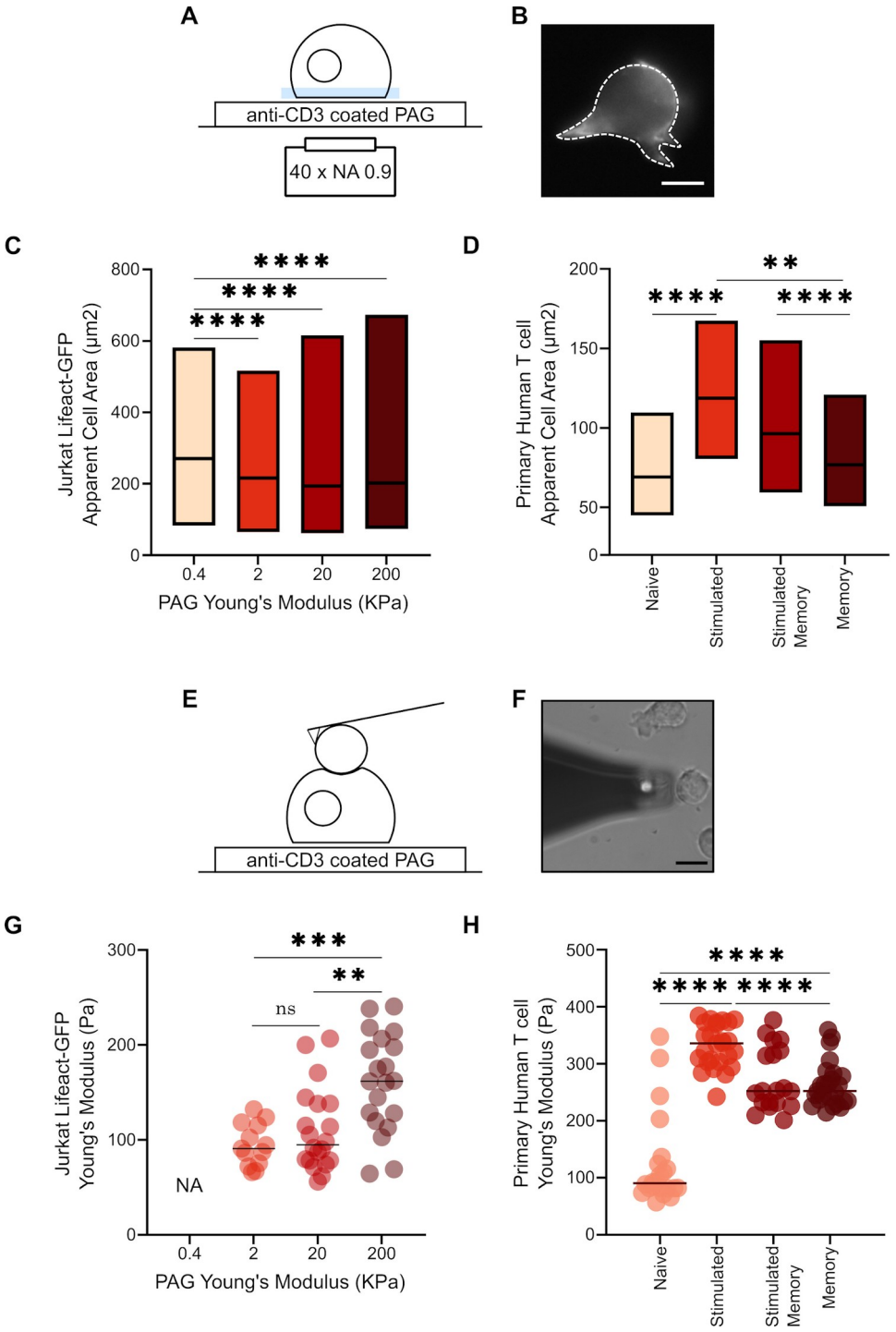
A
anti-CD3 coated PAG
40 x NA 0.9
B
C
Jurkat Lifeact-GFP
Apparent Cell Area (µm2)
800
600
400
200
0
****
****
****
0.4
2
20
200
PAG Young's Modulus (KPa)
D
Primary Human T cell
Apparent Cell Area (µm2)
200
150
100
50
0
**
****
****
Naive
Stimulated
Stimulated
Memory
Memory
E
anti-CD3 coated PAG
F
G
Jurkat Lifeact-GFP
Young's Modulus (Pa)
300
200
100
0
***
**
ns
NA
0.4
2
20
200
PAG Young's Modulus (KPa)
H
Primary Human T cell
Young's Modulus (Pa)
500
400
300
200
100
0
****
****
****
Naive
Stimulated
Stimulated
Memory
Memory

Figure 2

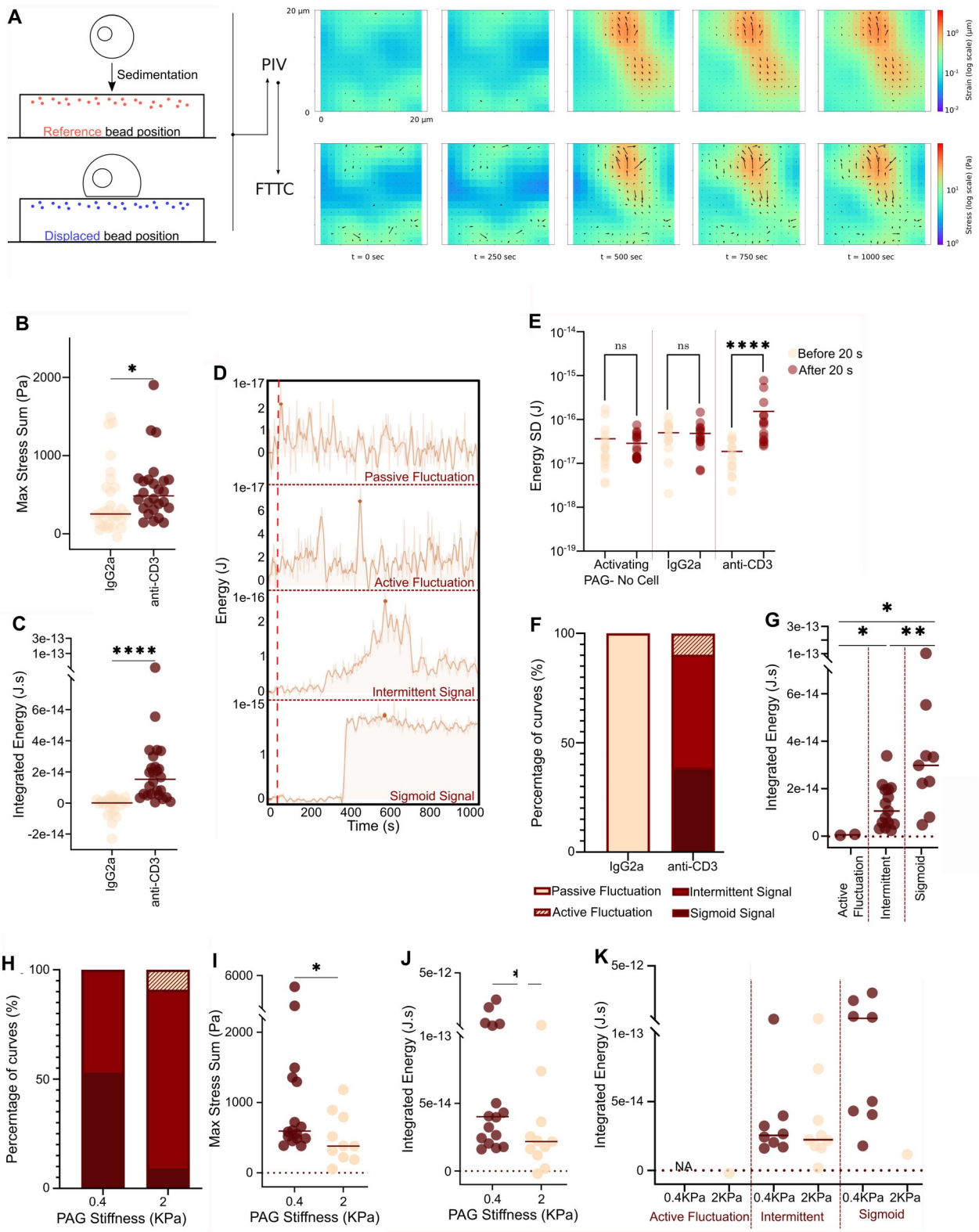
A
Sedimentation
Reference bead position
Displaced bead position
PIV
FTTC
20 µm
0
20 µm
Strain (log scale) (µm)
Stress (log scale) (Pa)
t = 0 sec
t = 250 sec
t = 500 sec
t = 750 sec
t = 1000 sec
B
Max Stress Sum (Pa)
IgG2a
anti-CD3
C
Integrated Energy (J.s)
IgG2a
anti-CD3
D
Energy (J)
Passive Fluctuation
Active Fluctuation
Intermittent Signal
Sigmoid Signal
Time (s)
E
Energy SD (J)
ns
ns
****
Before 20 s
After 20 s
Activating PAG- No Cell
IgG2a
anti-CD3
F
Percentage of curves (%)
IgG2a
anti-CD3
Passive Fluctuation
Active Fluctuation
Intermittent Signal
Sigmoid Signal
G
Integrated Energy (J.s)
Active Fluctuation
Intermittent
Sigmoid
H
Percentage of curves (%)
PAG Stiffness (KPa)
I
Max Stress Sum (Pa)
PAG Stiffness (KPa)
J
Integrated Energy (J.s)
PAG Stiffness (KPa)
K
Integrated Energy (J.s)
NA
0.4KPa 2KPa 0.4KPa 2KPa 0.4KPa 2KPa
Active Fluctuation
Intermittent
Sigmoid

Figure 3

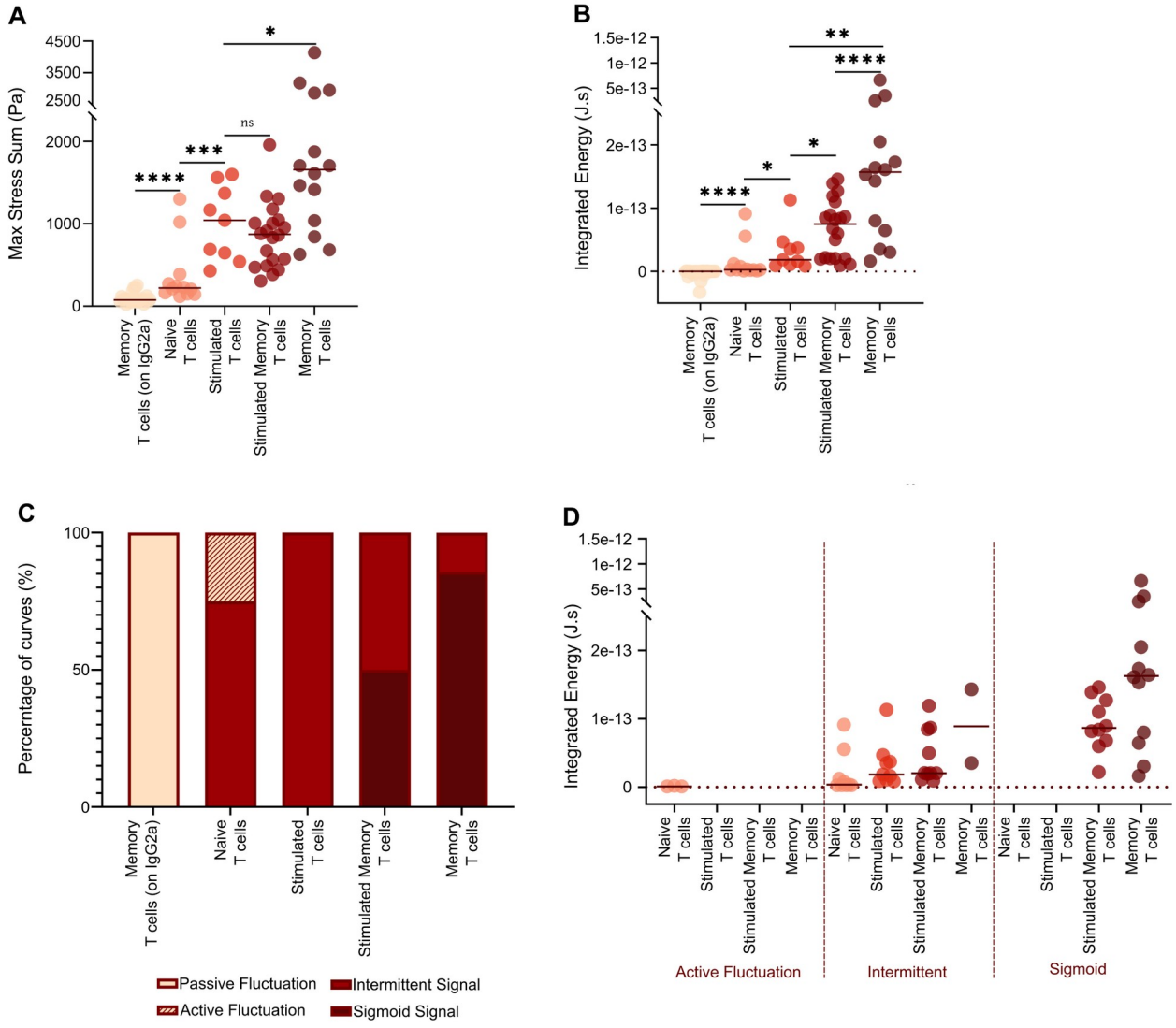
A
Max Stress Sum (Pa)
4500
3500
2500
2000
1000
0
****
***
ns
*
Memory T cells (on IgG2a)
Naive T cells
Stimulated T cells
Stimulated Memory T cells
Memory T cells
B
Integrated Energy (J.s)
1.5e-12
1e-12
5e-13
2e-13
1e-13
0
****
*
*
**
****
Memory T cells (on IgG2a)
Naive T cells
Stimulated T cells
Stimulated Memory T cells
Memory T cells
C
Percerntage of curves (%)
100
50
0
Memory T cells (on IgG2a)
Naive T cells
Stimulated T cells
Stimulated Memory T cells
Memory T cells
Passive Fluctuation
Intermittent Signal
Active Fluctuation
Sigmoid Signal
D
Integrated Energy (J.s)
1.5e-12
1e-12
5e-13
2e-13
1e-13
0
Naive T cells
Stimulated T cells
Stimulated Memory T cells
Memory T cells
Active Fluctuation
Intermittent
Sigmoid

Figure 4

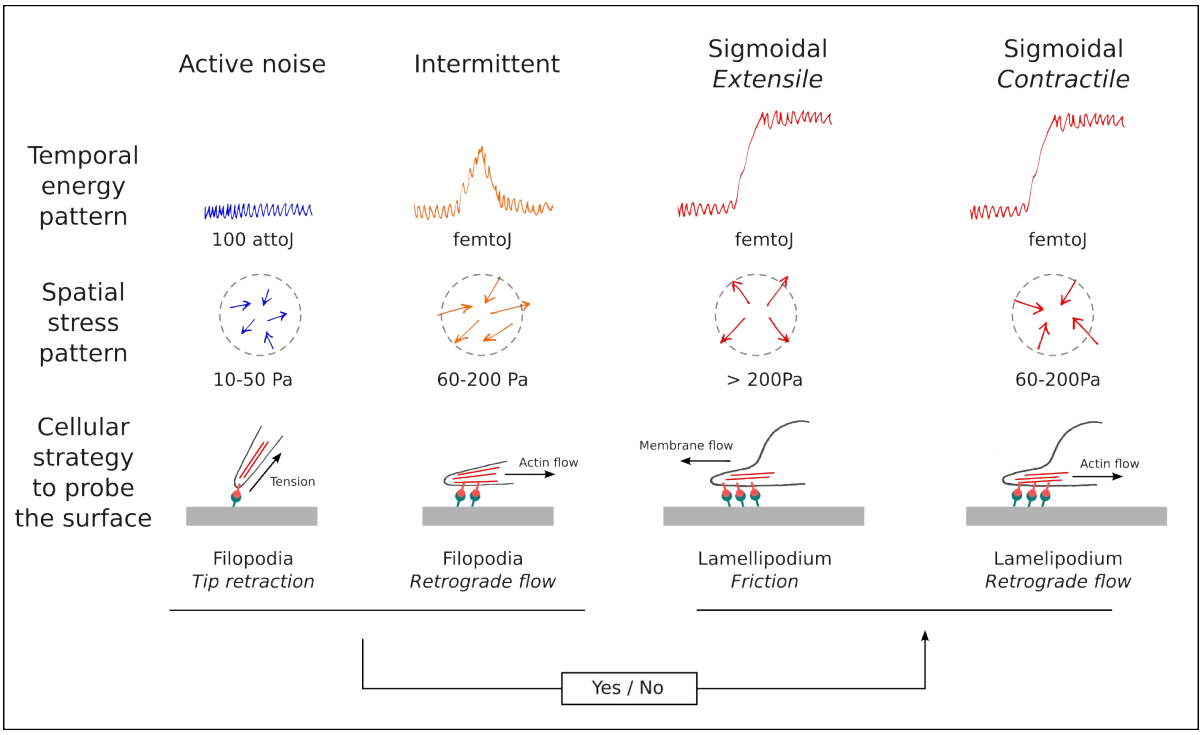
Active noise
Intermittent
Sigmoidal
Extensile
Sigmoidal
Contractile
Temporal energy pattern
100 attoJ
femtoJ
femtoJ
femtoJ
Spatial stress pattern
10-50 Pa
60-200 Pa
> 200Pa
60-200Pa
Cellular strategy to probe the surface
Tension
Actin flow
Membrane flow
Actin flow
Filopodia
Tip retraction
Filopodia
Retrograde flow
Lamellipodium
Friction
Lamelipodium
Retrograde flow
Yes / No

References

Alonso-Matilla, Roberto, Paolo P. Provenzano, and David J. Odde. 2023. 'Optimal Cell Traction Forces in a Generalized Motor-Clutch Model'. *Biophysical Journal* 122 (16): 3369–85. https://doi.org/10.1016/j.bpj.2023.07.012.

Babich, Alexander, Shuixing Li, Roddy S. O'Connor, Michael C. Milone, Bruce D. Freedman, and Janis K. Burkhardt. 2012. 'F-Actin Polymerization and Retrograde Flow Drive Sustained PLCγ1 Signaling during T Cell Activation'. *The Journal of Cell Biology* 197 (6): 775–87. https://doi.org/10.1083/jcb.201201018.

Bashour, K T, a Gondarenko, H Chen, et al. 2014. 'CD28 and CD3 Have Complementary Roles in T-Cell Traction Forces.' *Proceedings of the National Academy of Sciences* 111 (6): 2241–46. https://doi.org/10.1073/pnas.1315606111.

Basu, Roshni, and Morgan Huse. 2017. 'Mechanical Communication at the Immunological Synapse'. *Trends in Cell Biology* 27 (4): 241–54. https://doi.org/10.1016/j.tcb.2016.10.005.

Basu, Roshni, Benjamin M Whitlock, Julien Husson, et al. 2016. 'Cytotoxic T Cells Use Mechanical Force to Potentiate Target Cell Killing Cytotoxic T Cells Use Mechanical Force to Potentiate Target Cell Killing'. *Cell* 165 (1): 100–110. https://doi.org/10.1016/j.cell.2016.01.021.

Bergert, Martin, Anna Erzberger, Ravi A. Desai, et al. 2015. 'Force Transmission during Adhesion-Independent Migration'. *Nature Cell Biology* 17 (4): 524–29. https://doi.org/10.1038/ncb3134.

Bornschlögl, Thomas. 2013. 'How Filopodia Pull: What We Know about the Mechanics and Dynamics of Filopodia'. *Cytoskeleton* 70 (10): 590–603. https://doi.org/10.1002/cm.21130.

Brodovitch, Alexandre, Pierre Bongrand, and Anne Pierres. 2013. 'T Lymphocytes Sense Antigens within Seconds and Make a Decision within One Minute'. *Journal of Immunology (Baltimore, Md.: 1950)* 191 (5): 2064–71. https://doi.org/10.4049/jimmunol.1300523.

Brodovitch, Alexandre, Eugene Shenderov, Vincenzo Cerundolo, Pierre Bongrand, Anne Pierres, and Philip Anton van der Merwe. 2015. 'T Lymphocytes Need Less than 3 Min to Discriminate between Peptide MHCs with Similar TCR-Binding Parameters'. *European Journal of Immunology*, n/a-n/a. https://doi.org/10.1002/eji.201445214.

Bufi, Nathalie, Michael Saitakis, Stéphanie Dogniaux, et al. 2015. 'Human Primary Immune Cells Exhibit Distinct Mechanical Properties That Are Modified by Inflammation'. *Biophysical Journal* 108 (9): 2181–90. https://doi.org/10.1016/j.bpj.2015.03.047.

Burton, Kevin, Jung H Park, and D Lansing Taylor. 1999. 'Keratocytes Generate Traction Forces in Two Phases'. *Molecular Biology of the Cell* 10: 3745–69.

Butler, James P., Iva Marija Tolić-Nørrelykke, Ben Fabry, and Jeffrey J. Fredberg. 2002. 'Traction Fields, Moments, and Strain Energy That Cells Exert on Their Surroundings'. *American Journal of Physiology-Cell Physiology* 282 (3): C595–605. https://doi.org/10.1152/ajpcell.00270.2001.

Cai, En, Kyle Marchuk, Peter Beemiller, et al. 2017. 'Visualizing Dynamic Microvillar Search and Stabilization during Ligand Detection by T Cells'. *Science* 356 (6338): eaal3118–eaal3118. https://doi.org/10.1126/science.aal3118.

Cazaux, Séverine, Anaïs Sadoun, Martine Biarnes-Pelicot, et al. 2016. ‘Synchronizing Atomic Force Microscopy Force Mode and Fluorescence Microscopy in Real Time for Immune Cell Stimulation and Activation Studies’. *Ultramicroscopy* 160 (January): 168–81. https://doi.org/10.1016/j.ultramic.2015.10.014.

Chen, Yunfeng, Lining Ju, Muaz Rushdi, Chenghao Ge, and Cheng Zhu. 2017. ‘Receptor-Mediated Cell Mechanosensing’. *Molecular Biology of the Cell* 28 (23): 3134–55. https://doi.org/10.1091/mbc.E17-04-0228.

Clarke, D. Nathaniel, and Adam C. Martin. 2021. ‘Actin-Based Force Generation and Cell Adhesion in Tissue Morphogenesis’. *Current Biology* 31 (10): R667–80. https://doi.org/10.1016/j.cub.2021.03.031.

Colin-York, Huw, Yousef Javanmardi, Mark Skamrahl, et al. 2019. ‘Cytoskeletal Control of Antigen-Dependent T Cell Activation’. *Cell Reports* 26 (12): 3369-3379.e5. https://doi.org/10.1016/j.celrep.2019.02.074.

Comrie, William A., Alexander Babich, and Janis K. Burkhardt. 2015. ‘F-Actin Flow Drives Affinity Maturation and Spatial Organization of LFA-1 at the Immunological Synapse’. *The Journal of Cell Biology* 208 (4): 475–91. https://doi.org/10.1083/jcb.201406121.

Dillard, Pierre, Rajat Varma, Kheya Sengupta, and Laurent Limozin. 2014. ‘Ligand-Mediated Friction Determines Morphodynamics of Spreading T Cells’. *Biophysical Journal* 107 (11): 2629–38. https://doi.org/10.1016/j.bpj.2014.10.044.

Elosegui-Artola, Alberto, Roger Oria, Yunfeng Chen, et al. 2016. ‘Mechanical Regulation of a Molecular Clutch Defines Force Transmission and Transduction in Response to Matrix Rigidity’. *Nature Cell Biology* 18 (5): 540–48. https://doi.org/10.1038/ncb3336.

Engler, Adam J., Shamik Sen, H. Lee Sweeney, and Dennis E. Discher. 2006. ‘Matrix Elasticity Directs Stem Cell Lineage Specification’. *Cell* 126 (4): 677–89. https://doi.org/10.1016/j.cell.2006.06.044.

Geiger, B., and A. Bershadsky. 2001. ‘Assembly and Mechanosensory Function of Focal Contacts.’ *Curr Opin Cell Biol* 13 (5): 584–92.

Geiger, Benjamin, Joachim P. Spatz, and Alexander D. Bershadsky. 2009. ‘Environmental Sensing through Focal Adhesions’. *Nature Reviews Molecular Cell Biology* 10 (1): 21–33. https://doi.org/10.1038/nrm2593.

Göhring, Janett, Lukas Schrangl, Gerhard J. Schütz, and Johannes B. Huppa. 2022. ‘Mechanosurveillance: Tiptoeing T Cells’. *Frontiers in Immunology* 13 (May): 886328. https://doi.org/10.3389/fimmu.2022.886328.

Grakoui, A., S. K. Bromley, C. Sumen, et al. 1999. ‘The Immunological Synapse: A Molecular Machine Controlling T Cell Activation.’ *Science* 285 (5425): 221–27.

Henry, Steven J., Christopher S. Chen, John C. Crocker, and Daniel A. Hammer. 2015. ‘Protrusive and Contractile Forces of Spreading Human Neutrophils’. *Biophysical Journal* 109 (4): 699–709. https://doi.org/10.1016/j.bpj.2015.05.041.

Herant, M. 2006. ‘Mechanics of Neutrophil Phagocytosis: Experiments and Quantitative Models’. *Journal of Cell Science* 119 (9): 1903–13. https://doi.org/10.1242/jcs.02876.

Hivroz, Claire, and Michael Saitakis. 2016. ‘Biophysical Aspects of T Lymphocyte Activation at the Immune Synapse’. *Frontiers in Immunology* 7 (February). https://doi.org/10.3389/fimmu.2016.00046.

Hu, Kenneth H., and Manish J. Butte. 2016. ‘T Cell Activation Requires Force Generation’. *The Journal of Cell Biology* 213 (5): 535–42. https://doi.org/10.1083/jcb.201511053.

Hui, King Lam, Lakshmi Balagopalan, Lawrence E. Samelson, and Arpita Upadhyaya. 2015. ‘Cytoskeletal Forces during Signaling Activation in Jurkat T-Cells’. *Molecular Biology of the Cell* 26 (4): 685–95. https://doi.org/10.1091/mbc.E14-03-0830.

Hui, King Lam, and Arpita Upadhyaya. 2017. ‘Dynamic Microtubules Regulate Cellular Contractility during T-Cell Activation’. *Proceedings of the National Academy of Sciences* 114 (21): E4175–83. https://doi.org/10.1073/pnas.1614291114.

Huse, Morgan. 2017. ‘Mechanical Forces in the Immune System’. *Nature Reviews Immunology* 17 (11): 679–90. https://doi.org/10.1038/nri.2017.74.

Huse, Morgan. 2025. ‘Mechanoregulation of Lymphocyte Cytotoxicity’. *Nature Reviews Immunology* 25 (9): 680–95. https://doi.org/10.1038/s41577-025-01173-2.

Husson, Julien, Karine Chemin, Armelle Bohineust, Claire Hivroz, and Nelly Henry. 2011. ‘Force Generation upon T Cell Receptor Engagement’. *PLoS ONE* 6 (5): e19680. https://doi.org/10.1371/journal.pone.0019680.

Iwadate, Yoshiaki, and Shigehiko Yumura. 2008. ‘Molecular Dynamics and Forces of a Motile Cell Simultaneously Visualized by TIRF and Force Microscopies’. *BioTechniques* 44 (6): 739–50. https://doi.org/10.2144/000112752.

Jankowska, Katarzyna I., Edward K. Williamson, Nathan H. Roy, et al. 2018. ‘Integrins Modulate T Cell Receptor Signaling by Constraining Actin Flow at the Immunological Synapse’. *Frontiers in Immunology* 9 (January). https://doi.org/10.3389/fimmu.2018.00025.

Janmey, Paul A., Jessamine P. Winer, Maria E. Murray, and Qi Wen. 2009. ‘The Hard Life of Soft Cells’. *Cell Motility and the Cytoskeleton* 66 (8): 597–605. https://doi.org/10.1002/cm.20382.

Jannat, Risat A., Micah Dembo, and Daniel A. Hammer. 2011. ‘Traction Forces of Neutrophils Migrating on Compliant Substrates’. *Biophysical Journal* 101 (3): 575–84. https://doi.org/10.1016/j.bpj.2011.05.040.

Jaumouillé, Valentin, and Clare M. Waterman. 2020. ‘Physical Constraints and Forces Involved in Phagocytosis’. *Frontiers in Immunology* 11. https://doi.org/10.3389/fimmu.2020.01097.

Ju, Lining, Yunfeng Chen, Kaitao Li, et al. 2017. ‘Dual Biomembrane Force Probe Enables Single-Cell Mechanical Analysis of Signal Crosstalk between Multiple Molecular Species’. *Scientific Reports* 7 (1). https://doi.org/10.1038/s41598-017-13793-3.

Judokusumo, Edward, Erdem Tabdanov, Sudha Kumari, Michael L. Dustin, and Lance C. Kam. 2012. ‘Mechanosensing in T Lymphocyte Activation’. *Biophysical Journal* 102 (2): L5-7. https://doi.org/10.1016/j.bpj.2011.12.011.

Jung, Philipp, Xiangda Zhou, Sandra Iden, Markus Bischoff, and Bin Qu. 2021. ‘T Cell Stiffness Is Enhanced upon Formation of Immunological Synapse’. *eLife* 10 (July): e66643. https://doi.org/10.7554/eLife.66643.

Kaech, Susan M., Scott Hemby, Ellen Kersh, and Rafi Ahmed. 2002. ‘Molecular and Functional Profiling of Memory CD8 T Cell Differentiation’. *Cell* 111 (6): 837–51. https://doi.org/10.1016/s0092-8674(02)01139-x.

Kim, Sarah Hyun Ji, and Daniel A. Hammer. 2021. ‘Integrin Cross-Talk Modulates Stiffness-Independent Motility of CD4+ T Lymphocytes’. *Molecular Biology of the Cell* 32 (18): 1749–57. https://doi.org/10.1091/mbc.E21-03-0131.

Klotzsch, Enrico, and Gerhard J Schütz. 2013. ‘Improved Ligand Discrimination by Force-Induced Unbinding of the T Cell Receptor from Peptide-MHC.’ *Biophysical Journal* 104 (8): 1670–75. https://doi.org/10.1016/j.bpj.2013.03.023.

Kumari, Anita, Judith Pineau, Pablo J. Sáez, et al. 2019. ‘Actomyosin-Driven Force Patterning Controls Endocytosis at the Immune Synapse’. *Nature Communications* 10 (1): 2870. https://doi.org/10.1038/s41467-019-10751-7.

Lee, Moosung, Hyuntae Jeong, Chaeyeon Lee, et al. 2024. ‘High-Resolution Assessment of Multidimensional Cellular Mechanics Using Label-Free Refractive-Index Traction Force Microscopy’. *Communications Biology* 7 (1): 1. https://doi.org/10.1038/s42003-024-05788-4.

Li, Di, Huw Colin-York, Liliana Barbieri, et al. 2021. ‘Astigmatic Traction Force Microscopy (aTFM)’. *Nature Communications* 12 (1): 1. https://doi.org/10.1038/s41467-021-22376-w.

Limozin, Laurent, Marcus Bridge, Pierre Bongrand, Omer Dushek, Philip Anton van der Merwe, and Philippe Robert. 2019. ‘TCR-pMHC Kinetics under Force in a Cell-Free System Show No Intrinsic Catch Bond, but a Minimal Encounter Duration before Binding’. *Proceedings of the National Academy of Sciences of the United States of America* 116 (34): 16943–48. https://doi.org/10.1073/pnas.1902141116.

Limozin, Laurent, and Pierre-Henri Puech. 2019. ‘Membrane Organization and Physical Regulation of Lymphocyte Antigen Receptors: A Biophysicist’s Perspective’. *The Journal of Membrane Biology* 252 (4–5): 397–412. https://doi.org/10.1007/s00232-019-00085-2.

Liu, Baoyu, Elizabeth M. Kolawole, and Brian D. Evavold. 2021. ‘Mechanobiology of T Cell Activation: To Catch a Bond’. *Annual Review of Cell and Developmental Biology* 37 (1): 65–87. https://doi.org/10.1146/annurev-cellbio-120219-055100.

Liu, K., Y. Li, V. Prabhu, et al. 2001. ‘Augmentation in Expression of Activation-Induced Genes Differentiates Memory from Naive CD4+ T Cells and Is a Molecular Mechanism for Enhanced Cellular Response of Memory CD4+ T Cells’. *Journal of Immunology (Baltimore, Md.: 1950)* 166 (12): 7335–44. https://doi.org/10.4049/jimmunol.166.12.7335.

Liu, Yang, Lori Blanchfield, Victor Pui-Yan Ma, et al. 2016. ‘DNA-Based Nanoparticle Tension Sensors Reveal That T-Cell Receptors Transmit Defined pN Forces to Their Antigens for Enhanced Fidelity’. *Proceedings of the National Academy of Sciences* 113 (20): 5610–15. https://doi.org/10.1073/pnas.1600163113.

Ma, Rong, Anna V. Kellner, Victor Pui-Yan Ma, et al. 2019. ‘DNA Probes That Store Mechanical Information Reveal Transient Piconewton Forces Applied by T Cells’. Biological Sciences.

Proceedings of the National Academy of Sciences 116 (34): 16949–54. https://doi.org/10.1073/pnas.1904034116.

Martiel, Jean-Louis, Aldo Leal, Laetitia Kurzawa, et al. 2015. ‘Measurement of Cell Traction Forces with ImageJ’. In *Methods in Cell Biology*, vol. 125. Elsevier. https://doi.org/10.1016/bs.mcb.2014.10.008.

Martino, Fabiana, Ana R. Perestrelo, Vladimír Vinarský, Stefania Pagliari, and Giancarlo Forte. 2018. ‘Cellular Mechanotransduction: From Tension to Function’. *Frontiers in Physiology* 9. https://www.frontiersin.org/article/10.3389/fphys.2018.00824.

Monks, Colin R. F., Benjamin A. Freiberg, Hannah Kupfer, Noah Sciaky, and Abraham Kupfer. 1998. ‘Three-Dimensional Segregation of Supramolecular Activation Clusters in T Cells’. *Nature* 395 (6697): 82–86. https://doi.org/10.1038/25764.

Murphy, Kenneth M., Casey Weaver, Leslie J. Berg, and Charles A. Janeway. 2022. *Janeway’s Immunobiology*. 10th edition, International student edition. With Gregory Barton. W.W. Norton & Company.

Mustapha, Farah, Kheya Sengupta, and Pierre-Henri Puech. 2022. ‘Protocol for Measuring Weak Cellular Traction Forces Using Well-Controlled Ultra-Soft Polyacrylamide Gels’. *STAR Protocols* 3 (1): 101133. https://doi.org/10.1016/j.xpro.2022.101133.

O’Connor, Roddy S, Xueli Hao, Keyue Shen, et al. 2012. ‘Substrate Rigidity Regulates Human T Cell Activation and Proliferation.’ *Journal of Immunology (Baltimore, Md. : 1950)* 189 (3): 1330–39. https://doi.org/10.4049/jimmunol.1102757.

Paluch, Ewa K., Irene M. Aspalter, and Michael Sixt. 2016. ‘Focal Adhesion-Independent Cell Migration’. *Annual Review of Cell and Developmental Biology* 32 (October): 469–90. https://doi.org/10.1146/annurev-cellbio-111315-125341.

Pang, Ruiyang, Weihao Sun, Yingyun Yang, et al. 2024. ‘PIEZO1 Mechanically Regulates the Antitumour Cytotoxicity of T Lymphocytes’. *Nature Biomedical Engineering*, March 21, 1–15. https://doi.org/10.1038/s41551-024-01188-5.

Parr, Avery, Nicholas R. Anderson, and Daniel A. Hammer. 2019. ‘A Simulation of the Random and Directed Motion of Dendritic Cells in Chemokine Fields’. *PLOS Computational Biology* 15 (10): e1007295. https://doi.org/10.1371/journal.pcbi.1007295.

Pathni, Aashli, Altuğ Özçelikkale, Ivan Rey-Suarez, et al. 2022. ‘Cytotoxic T Lymphocyte Activation Signals Modulate Cytoskeletal Dynamics and Mechanical Force Generation’. *Frontiers in Immunology* 13: 779888. https://doi.org/10.3389/fimmu.2022.779888.

Pelham, Robert J., and Yu-li Wang. 1997. ‘Cell Locomotion and Focal Adhesions Are Regulated by Substrate Flexibility’. Biological Sciences. *Proceedings of the National Academy of Sciences* 94 (25): 13661–65. https://doi.org/10.1073/pnas.94.25.13661.

Pierres, Anne, Anne-Marie Benoliel, Dominique Touchard, and Pierre Bongrand. 2008. ‘How Cells Tiptoe on Adhesive Surfaces before Sticking.’ *Biophysical Journal* 94 (10): 4114–22. https://doi.org/10.1529/biophysj.107.125278.

Puech, Pierre-Henri, and Pierre Bongrand. 2021. ‘Mechanotransduction as a Major Driver of Cell Behaviour: Mechanisms, and Relevance to Cell Organization and Future Research’. *Open Biology* 11 (11): 210256. https://doi.org/10.1098/rsob.210256.

Puech, Pierre-Henri, Damien Nevoltris, Philippe Robert, Laurent Limozin, Claude Boyer, and Pierre Bongrand. 2011. ‘Force Measurements of TCR/pMHC Recognition at T Cell Surface’. *PLoS ONE* 6 (7): e22344. https://doi.org/10.1371/journal.pone.0022344.

Reichardt, Peter, Bastian Dornbach, and Matthias Gunzer. 2010. ‘APC, T Cells, and the Immune Synapse’. *Current Topics in Microbiology and Immunology* 340: 229–49. https://doi.org/10.1007/978-3-642-03858-7_12.

Rheinlaender, Johannes, Andrea Dimitracopoulos, Bernhard Wallmeyer, et al. 2020. ‘Cortical Cell Stiffness Is Independent of Substrate Mechanics’. *Nature Materials* 19 (9): 1019–25. https://doi.org/10.1038/s41563-020-0684-x.

Ricart, Brendon G., Michael T. Yang, Christopher A. Hunter, Christopher S. Chen, and Daniel A. Hammer. 2011. ‘Measuring Traction Forces of Motile Dendritic Cells on Micropost Arrays’. *Biophysical Journal* 101 (11): 2620–28. https://doi.org/10.1016/j.bpj.2011.09.022.

Ronceray, Pierre, and Martin Lenz. 2015. ‘Connecting Local Active Forces to Macroscopic Stress in Elastic Media’. *Soft Matter* 11 (8): 1597–605. https://doi.org/10.1039/C4SM02526A.

Sadoun, Anaïs, Martine Biarnes-Pelicot, Laura Ghesquiere-Dierickx, et al. 2021. ‘Controlling T Cells Spreading, Mechanics and Activation by Micropatterning’. *Scientific Reports* 11 (1): 6783. https://doi.org/10.1038/s41598-021-86133-1.

Saitakis, Michael, Stéphanie Dogniaux, Christel Goudot, et al. 2017. ‘Different TCR-Induced T Lymphocyte Responses Are Potentiated by Stiffness with Variable Sensitivity’. *eLife* 6 (June). https://doi.org/10.7554/eLife.23190.

Sawicka, Anna, Avin Babataheri, Stéphanie Dogniaux, et al. 2017. ‘Micropipette Force Probe to Quantify Single-Cell Force Generation: Application to T-Cell Activation’. *Molecular Biology of the Cell* 28 (23): 3229–39. https://doi.org/10.1091/mbc.E17-06-0385.

Schwarz, Ulrich S., and Samuel A. Safran. 2013. ‘Physics of Adherent Cells’. *Reviews of Modern Physics* 85 (3): 1327–81. https://doi.org/10.1103/RevModPhys.85.1327.

Sengupta, Kheya, Pierre Dillard, and Laurent Limozin. 2024. ‘Morphodynamics of T-Lymphocytes: Scanning to Spreading’. *Biophysical Journal*, February, S0006349524001577. https://doi.org/10.1016/j.bpj.2024.02.023.

Solon, Jérôme, Ilya Levental, Kheya Sengupta, Penelope C. Georges, and Paul A. Janmey. 2007. ‘Fibroblast Adaptation and Stiffness Matching to Soft Elastic Substrates’. *Biophysical Journal* 93 (12): 4453–61. https://doi.org/10.1529/biophysj.106.101386.

Spillane, Katelyn M., and Pavel Tolar. 2018. ‘Mechanics of Antigen Extraction in the B Cell Synapse’. *Molecular Immunology* 101 (September): 319–28. https://doi.org/10.1016/j.molimm.2018.07.018.

Tanimoto, Hirokazu, and Masaki Sano. 2014. ‘A Simple Force-Motion Relation for Migrating Cells Revealed by Multipole Analysis of Traction Stress’. *Biophysical Journal* 106 (1): 16–25. https://doi.org/10.1016/j.bpj.2013.10.041.

Thauland, Timothy J., Kenneth H. Hu, Marc A. Bruce, and Manish J. Butte. 2017. ‘Cytoskeletal Adaptivity Regulates T Cell Receptor Signaling’. *Science Signaling* 10 (469): eaah3737. https://doi.org/10.1126/scisignal.aah3737.

Tinevez, Jean-Yves, Nick Perry, Johannes Schindelin, et al. 2017. ‘TrackMate: An Open and Extensible Platform for Single-Particle Tracking’. *Methods (San Diego, Calif.)* 115 (February): 80–90. https://doi.org/10.1016/j.ymeth.2016.09.016.

Tse, Justin R., and Adam J. Engler. 2010. ‘Preparation of Hydrogel Substrates with Tunable Mechanical Properties’. *Current Protocols in Cell Biology* 47 (1): 10.16.1-10.16.16. https://doi.org/10.1002/0471143030.cb1016s47.

Vitiello, Elisa, Laura Andreina Chaco, Martial Balland, and Kalpana Mandal. 2014. *Cell Dipole Behaviour Revealed by ECM Sub-Cellular Geometry*. https://doi.org/10.1038/ncomms6749.

Vogel, Viola, and Michael Sheetz. 2006. ‘Local Force and Geometry Sensing Regulate Cell Functions’. *Nature Reviews Molecular Cell Biology* 7 (4): 265–75. https://doi.org/10.1038/nrm1890.

Vorselen, Daan, Sarah R Barger, Yifan Wang, et al. 2021. ‘Phagocytic “Teeth” and Myosin-II “Jaw” Power Target Constriction during Phagocytosis’. *eLife* 10 (October): e68627. https://doi.org/10.7554/eLife.68627.

Vorselen, Daan, Yifan Wang, Miguel M. de Jesus, et al. 2020. ‘Microparticle Traction Force Microscopy Reveals Subcellular Force Exertion Patterns in Immune Cell–Target Interactions’. *Nature Communications* 11 (1). https://doi.org/10.1038/s41467-019-13804-z.

Wahl, Astrid, Céline Dinet, Pierre Dillard, et al. 2019. ‘Biphasic Mechanosensitivity of T Cell Receptor-Mediated Spreading of Lymphocytes’. *Proceedings of the National Academy of Sciences* 116 (13): 5908–13. https://doi.org/10.1073/pnas.1811516116.

Yuan, Dennis J., Lingting Shi, and Lance C. Kam. 2021. ‘Biphasic Response of T Cell Activation to Substrate Stiffness’. *Biomaterials* 273 (June): 120797. https://doi.org/10.1016/j.biomaterials.2021.120797.

Zak, Alexandra, Sara Violeta Merino-Cortés, Anaïs Sadoun, et al. 2021. ‘Rapid Viscoelastic Changes Are a Hallmark of Early Leukocyte Activation’. *Biophysical Journal* 120 (9): 1692–704. https://doi.org/10.1016/j.bpj.2021.02.042.